



Radiotolerant endophytic bacteria and analysis of the effects of $^{137}\text{Cesium}$ on the metabolome of *Pantoea* sp.

João Arthur dos Santos Oliveira¹ · Andressa Domingos Polli¹ · Ana Paula Ferreira¹ · Nilson Benedito Lopes² ·
Claudete Aparecida Mangolim¹ · Veronica Elisa Pimenta Vicentini¹ · Julio Cesar Polonio¹  ·
Anderson Valdiney Gomes Ramos³ · Debora Cristina Baldoqui³ · João Alencar Pamphile¹ · João Lucio Azevedo⁴

Received: 2 April 2024 / Accepted: 10 July 2024 / Published online: 31 July 2024
© The Author(s) under exclusive licence to Sociedade Brasileira de Microbiologia 2024

Abstract

Some bacteria have developed mechanisms to withstand the stress caused by ionizing radiation. The ability of these radio-resistant microorganisms to survive high levels of radiation is primarily attributed to their DNA repair mechanisms and the production of protective metabolites. To determine the effect of irradiation on bacterial growth, we propose to compare the metabolites produced by the irradiated isolates to those of the control (non-irradiated isolates) using mass spectrometry, molecular networking, and chemometric analysis. We identified the secondary metabolites produced by these bacteria and observed variations in growth following irradiation. Notably, after 48 h of exposure to radiation, *Pantoea* sp. bacterial cells exhibited a significant 6-log increase compared to non-irradiated cells. Non-irradiated cells produce exclusively Pyridindolol, 1-hydroxy-4-methylcarbostyryl, N-alkyl, and N-2-alkoxyethyl diethanolamine, while 5'-methylthioadenosine was detected only in irradiated cells. These findings suggest that the metabolic profile of *Pantoea* sp. remained relatively stable. The results obtained from this study have the potential to facilitate the development of innovative strategies for harnessing the capabilities of endophytic bacteria in radiological protection and bioremediation of radionuclides.

Keywords Gamma radiation · Endophytic bacteria, Radiotolerance · Metabolome · Molecular networking

Introduction

Following the nuclear accidents at Chernobyl (1986) and Fukushima Daiichi (2011), increased attention has been paid to the environmental and human health impacts of exposure to radioactive materials [1]. Radionuclides, such as ^{40}K , ^{137}Cs , ^{226}Ra , ^{228}Ra , and ^{232}Th , occur in rock formations and chemical fertilizers and can originate from mining activities or nuclear accidents [2]. These radionuclides are harmful and generally occur in different concentrations in the environment [3]. Therefore, it is important to understand the behavior and concentrations of radionuclides in the environment for developing strategies for protecting human health and the ecosystem [2].

$^{137}\text{Cesium}$ (half-life ± 30 years) is an artificial radionuclide that can be released into the environment following nuclear weapons tests and/or accidents at nuclear power plants [3]. The largest nuclear accident involving ^{137}Cs occurred in the city of Goiânia (Goiás) in Brazil in 1987. The accident exposed thousands of people to the ionizing

João Alencar Pamphile: In memoriam

Responsible Editor: Lucy Seldin

✉ Julio Cesar Polonio
jcpolonio2@uem.br

¹ Department of Biotechnology, Genetics, and Cell Biology, State University of Maringá, Maringá, Paraná 87020-900, Brazil

² Department of Physics, State University of Maringá, Maringá, Paraná 87020-900, Brazil

³ Department of Chemistry, State University of Maringá, Maringá, Paraná 87020-900, Brazil

⁴ Department of Genetics, Superior College of Agriculture (Luiz de Queiroz), University of São Paulo, Piracicaba, São Paulo 13418-900, Brazil

radiation emitted by the material, resulting in the death of many people [4, 5].

Gamma rays emitted by radionuclides and other materials are examples of ionizing radiation. This type of radiation is an electromagnetic wave that results in oxidative stress and damages genetic material [6]. However, some organisms, such as bacteria and fungi, can withstand high levels of exposure to this type of ionizing radiation, which in many cases is lethal to other organisms [7].

The ability of these so-called “radioresistant” microorganisms to survive high radiation levels has been studied and is mainly associated with particular DNA repair mechanisms and the ability of these microorganisms to produce primary and/or secondary metabolites that act against the stress caused by the ionizing radiation [8, 9].

Endophytic microorganisms, which associate internally with plant tissues in an asymptomatic manner [10], have applications in different areas, including agriculture, where they promote plant growth [11], and in industry, where they produce enzymes [12] or bioactive metabolites [13]. These microorganisms can also act as remediation agents at sites contaminated with radioactive materials [14]. Endophytic bacterial consortia have demonstrated an increase of up to 90% in the volume of radionuclides and heavy metals in host plants in contaminated soils [15].

The interactions between microorganisms and radiation for biotechnological purposes have not been properly explored [7]; therefore, it is important to study the radioresistance/sensitivity of these microorganisms to radionuclides, such as ^{137}Cs , that emit ionizing radiation to get a better understanding of the interaction and the protective/repair mechanisms that they possess to identify those with potential bioremediation roles at sites directly or indirectly contaminated with radioactive materials or to develop new biomaterials that can be used as radiological protection mechanisms.

This study investigated the radiotolerance of four endophytic bacteria to the ionizing radiation emitted by a ^{137}Cs source. Culture-dependent methods, such as broth microdilution, were used to determine differences in bacterial growth between irradiated and non-irradiated cells. Metabolites produced by bacterial isolates that showed differences in growth after irradiation were compared with metabolites from control (non-irradiated) isolates using mass spectrometry, molecular networking, and chemometric analysis.

Materials and methods

Endophytic bacteria

The endophytic bacteria *Pantoea* sp. ELP04, *Pantoea* sp. ELP01, *Erwinia* sp. ELP06, and *Pantoea* sp. ELG24 were

isolated from the ornamental plant *Echeveria laui* (Saxifragales: Crassulaceae) [11] obtained from the Collection of Endophytic and Environmental Microorganisms (CMEA) at the Laboratory of Microbial Biotechnology (LBIOMIC) of the State University of Maringá (Paraná, Brazil). The use of these isolates was registered at the Council for Genetic Heritage Management (SisGen: A401F1E). The bacterial isolates were initially preserved in 25% glycerol in trypticase soy broth (TSB; pH 7.3) medium and maintained at -80 °C. They were reactivated using TSB medium (pH 7.3) for 48 h at 28 °C, transferred to trypticase soy agar (TSA; pH 7.3) medium, and grown for 24 h at 28 °C. Their sensitivity to ionizing radiation was then evaluated.

Ionizing radiation sensitivity test

The bacteria were cultivated in TSB medium (pH 7.3) at 28 °C for 24 h. A 20 µL bacterial suspension standardized using a spectrophotometer (600 nm optical density of 0.2) was added to a 96-well microdilution plate containing 180 µL TSB medium (Fig. 1). Gamma radiation experiments were performed at the Nuclear Physics Laboratory (Physics Department of the State University of Maringá, Paraná, Brazil) accredited by the National Nuclear Energy Commission (CNEN; number 13,361).

The bacterial suspension was irradiated with gamma rays emitted by the ^{137}Cs source (50 mCi activity) at a distance of 7 cm for 24 h and 48 h, with final doses of 0.72 Gy and 1.45 Gy, respectively. A microdilution plate not exposed to gamma radiation was used as a control to study the growth of each bacterial isolate. After exposure, aliquots were taken, diluted in TSB medium (1:10), seeded (5 µL) on solid TSA (pH 7.3), and then incubated at 28 °C for 24 h (Fig. 1).

Colony forming unit (CFU) counts were performed in triplicates and the results compared using analysis of variance implemented in SISVAR v.5.6. Aliquots of the treated and control bacteria were subjected to scanning electron microscopy (SEM) at the research support center complex (COMCAP) of the State University of Maringá (Paraná, Brazil).

Obtaining metabolic extracts

Metabolites produced by *Pantoea* sp. ELP04 were analyzed. The bacterium was chosen based on the results of the radiation sensitivity test (Table 1). Metabolites were obtained from bacterial cells exposed to radiation for 48 h. A microbial growth curve was initially generated to identify the isolate's log growth phase. After pre-growth, the optical density was adjusted to 0.2 (at 600 nm) using 0.85% saline (NaCl). The adjusted inoculum (1 mL) was added to 14 mL TSB medium (pH 7.3) and incubated at 28 °C with agitation

Fig. 1 Test of sensitivity to ionizing radiation using a 96-well microdilution plate

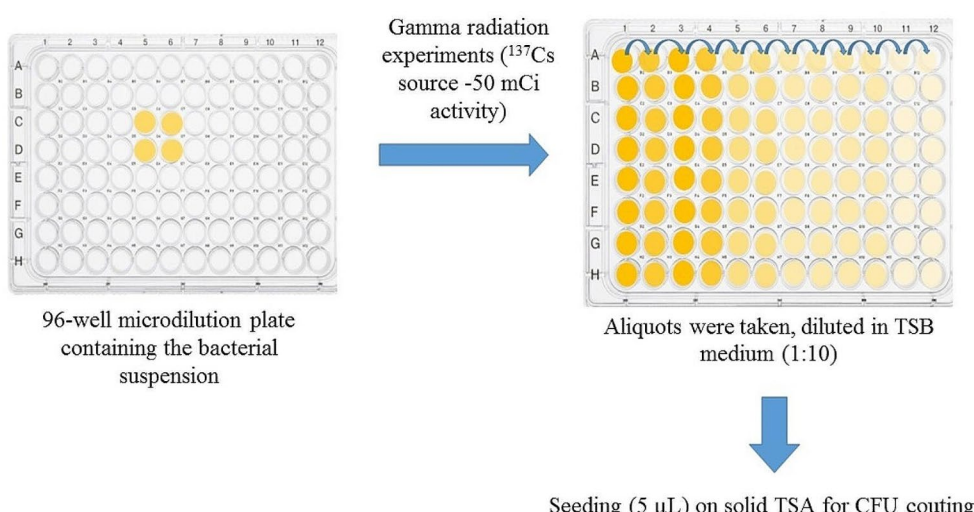


Table 1 Gamma radiation sensitivity screening of endophytic bacterial isolates from *Echeveria laui*. Final doses 24 h (0.72 Gy) and 48 h (1.45 Gy)

Bacteria	Treatments					
	24 h control*	24 h*	Variation**	48 h control*	48 h*	Variation**
<i>Pantoea</i> sp. ELP01	9.74 ± 0.03	12.71 ± 0.21	2.97	13.32 ± 0.08	11.23 ± 0.06	-2.09
<i>Pantoea</i> sp. ELP04	19.63 ± 0.16	21.69 ± 0.05	2.06	30.87 ± 0.02	36.92 ± 0.03	6.05
<i>Erwinia</i> sp. ELP06	15.71 ± 0.06	>16	+	13.69 ± 0.04	11.76 ± 0.03	-1.93
<i>Pantoea</i> sp. ELG24	13.76 ± 0.09	>16	+	25.56 ± 0.03	28.65 ± 0.07	3.09

*Means in Log CFU.mL⁻¹; ** Log CFU.mL⁻¹ in relation to the control

at 150 rpm. Optical density readings were taken over 11 h at 30–30 min intervals to generate the growth curve (data not shown).

After generating the microbial growth curve, 10 mL of the adjusted *Pantoea* sp. ELP04 suspension (600 nm = 0.2), irradiated for 48 h, was added to 90 mL of TSB medium (pH 7.3). The mixture was then incubated with agitation at 150 rpm and 28 °C for 9 h. The same procedure was performed for the non-irradiated control isolate and for the TSB culture medium containing no bacterial inoculum. The treatments were designated as follows: F3 for metabolites obtained from the irradiated bacteria, F2 for metabolites from the control bacteria (non-irradiated), and F1 for the negative control (culture medium with no microbial inoculum).

To obtain the ethyl acetate fraction (EtOAc), the cultured products and control were centrifuged at 16,000 g for 15 min to separate bacterial cells (F2 and F3). Cultured products (F2 and F3) and control (F1) were extracted through liquid–liquid partition in a separating funnel using the organic solvent ethyl acetate in a 1:5 ratio (ethyl acetate: medium). The experiment was conducted in triplicates. The resulting solvent was treated with sodium sulfate for 24 h and then subjected to rotary evaporation to obtain EtOAc fractions containing metabolites, as described by Oliveira et al. [16].

For the methanol fraction (MeOH), the cultured products were centrifuged at 16,000 g for 15 min to separate cells.

The resulting bacterial cell mass was combined with 30 mL of methanol in 50 mL centrifuge tubes, vortexed to generate a homogenate, and placed in an ultrasonic bath for 15 min at room temperature (± 28 °C). The solution was then centrifuged at 16,000 g for 15 min and the resulting methanol collected. The experiment was conducted in triplicates, and the methanol fraction collected from each replicate was collected and subjected to rotary evaporation, as described above.

Ultra-high-performance liquid chromatography-tandem mass spectrometry analysis (UPLC-HRMS)

The extracts were solubilized in methanol (1.0 mg.mL⁻¹), centrifuged, and were analyzed using ultra-high-performance liquid chromatography (Shimadzu, Nexera X2, Japan) coupled to a quadrupole time-of-flight high-resolution mass spectrometer (Q-TOF) (Impact II, Bruker Daltonics Corporation, Germany) (resolution of > 60,000) equipped with an electrospray ionization source (ESI).

Chromatographic separation was performed using a C18 column (75 × 2.0 mm i.d.; Shim-pack XR-ODS III at 1.6 M). The mixture of solvents A (H₂O) and B (acetonitrile with 0.1% formic acid; v:v) was separated on a gradient using the following parameters: 5% B for 0–1 min, 30% B for 1–3 min, 95% B for 3–12 min, held at 95% B for 12–15 min and 5% B for 15–17 min at 40 °C. Zero point 1% of formic

acid was added to the organic solvent to analyze the positive ionization mode, while pure acetonitrile was used for the negative mode. Flow rate and sample injection volume were set at $0.2 \text{ mL} \cdot \text{min}^{-1}$ and $3 \mu\text{L}$, respectively. Capillary voltage was operated in positive and negative ionization modes set to 4,500 V, with an endplate compensation potential of -500 V. Gas parameters were set to $8 \text{ L} \cdot \text{min}^{-1}$ at 200°C , with nebulizing gas pressure of 4 bar. Data were collected between m/z 50–1400, with an acquisition rate of 5 spectra per second, and ions of interest were selected by automatic MS/MS fragmentation. The data were processed using data analysis software v.4.3 (Bruker).

Molecular networking and chemometric analysis

To conduct molecular networking analyses, raw data from EtOAc and MeOH fractions obtained from the UPLC-HR-MS/MS were converted to “.mzXML” file format in the data analysis software (Bruker) and clustered using the MS-Cluster algorithm in the global natural products social (GNPS) [17]. A molecular network was generated using the online workflow (<https://ccms-ucsd.github.io/GNPSDocumentation/>) on the GNPS website (<http://gnps.ucsd.edu>). Data were filtered by removing all MS/MS fragment ions within ± 17 Da of the m/z precursor. The MS/MS spectra were window-filtered by choosing only the top six fragment ions in the ± 50 Da window across the spectrum.

The precursor ion mass tolerance and MS/MS fragment ion tolerance were each set to 0.02 Da. A network was subsequently generated where edges were filtered to have a cosine score above 0.7 and more than five matching peaks. Edges between two nodes were kept in the network only if each of the nodes appeared in the top 10 most similar nodes.

The maximum size of a molecular family was set to 100; thus, the lowest-scoring border was removed until the molecular family size was below this limit. The spectra of the network were then searched in Global Natural Products Social Network Analysis spectral libraries (GNPS). The library spectra were filtered in the same manner as the input data. All matches between the network and library spectra were required to have a score above 0.7 and at least five matching peaks. Finally, the spectra were imported into Cytoscape (version 3.8.1) for visualization [18]. Compounds were putatively identified based on literature data [19, 20] and by comparing the spectra and fragmentation patterns of the ions obtained with those available in MassBank (<http://www.massbank.jp/>) and GNPS (<http://gnps.ucsd.edu>) databases.

MarkerLynx (V4.1) was used to select target ions for chemometric analysis using an ion exclusion list (those detected in the mobile phase). The resulting ions were normalized using Pareto scaling. Normalized data were analyzed using

multivariate statistical techniques with unsupervised and supervised approaches, such as principal component analysis (PCA), and discriminant analyses, such as projections for discriminant analysis of latent structures (PLS-DA) and orthogonal projections for discriminant analysis of latent structures (OPLS-DA). Heatmaps were generated to visualize the output of discriminant analyses. Analyses were conducted using MetaboAnalyst 4.0, an online statistical platform, and MarkerLynx XS v.3.0.1.0.

Results and discussion

Radiation sensitivity test

Results of the sensitivity of the endophytic bacteria *Pantoea* sp. ELP04, *Pantoea* sp. ELP01, *Erwinia* sp. ELP06, and *Pantoea* sp. ELG24 to radiation emitted by ^{137}Cs are presented in Table 1. After 24 h, the four isolates showed growth variations compared with their respective controls, with *Erwinia* sp. ELP06 and *Pantoea* sp. ELG24 showing the largest differences ($> 16 \text{ Log CFU} \cdot \text{mL}^{-1}$). However, the growth of *Pantoea* sp. ELP01, *Erwinia* sp. ELP06, and *Pantoea* sp. ELG24 after 48 h was lower than the growth recorded at 24 h. Although *Pantoea* sp. ELG24 had a $> 3 \text{ Log CFU} \cdot \text{mL}^{-1}$ difference in growth compared with the control, there was a decrease of approximately $12 \text{ Log CFU} \cdot \text{mL}^{-1}$ between its growth at 24 and 48 h. Only *Pantoea* sp. ELP04 showed higher growth at 48 h than that at 24 h ($> 4 \text{ Log CFU} \cdot \text{mL}^{-1}$) (Fig. S1). Due to the differential growth observed in both periods analyzed (24 and 48 h), the isolate ELP04 was selected for further studies on its radiotolerance potential, with a particular emphasis on its metabolome.

SEM showed slightly elongated rod-shaped and non-encapsulated cells, a normal morphological characteristic for bacteria of the genus *Pantoea* [21]. No visible external morphological differences were observed between bacteria that were not exposed to gamma radiation (Fig. S2a) and those that were exposed to gamma radiation (Fig. S2b).

Microorganisms, particularly bacteria, comprise agents with potential biotechnological properties for the bioremediation of sites contaminated with radioactive materials [14, 22–26]. Some genera, including *Methylobacterium* sp., *Bacillus* sp., *Pseudomonas* sp., *Nocardia* sp., *Deinococcus* sp., *Micrococcus* sp., and *Staphylococcus* sp. [27–30], have been isolated from environments contaminated with nuclear waste, suggesting that these microorganisms are at least radiotolerant to ionizing radiation. To the best of our knowledge, there are no reports on the sensitivity or resistance of bacteria in the genus *Pantoea* to ionizing radiation emitted by nuclear materials, particularly ^{137}Cs .

These radioactive materials may be captured and/or accumulated by microorganisms because many of the elements show chemical characteristics similar to those of essential nutrients and, when captured, are assimilated erroneously. Thus, these organisms can help reduce the concentration of these agents in the environment by sequestering them [31], as shown in *Pseudomonas* sp. [30] and *Streptomyces* sp. [32].

Oxidative stress caused by ionizing radiation can result in abnormal production of peroxides and free radicals that damage DNA [33]. The mechanisms available to the cell to combat radiation-induced oxidative stress are important indicators of its sensitivity or resistance [31] and include the production of metabolites that act against this stress [8, 9].

Chemical analysis of fermented products

Molecular networking results of the EtOAc and MeOH extracts are shown in Fig. 2 and Fig. S30–S33. The two extracts contained similar metabolites (EtOAc × EtOAc/MeOH × MeOH and EtOAc × MeOH), from which it was possible to generate families (clusters). We analyzed 10,593 spectra with 990 nodes and 995 pairs.

Analysis of different databases, including MassBank, as well as information available on GNPS, identified putatively 24 compounds. A summary of these compounds and their presence (+) or absence (-) in the extracts is presented in Table 2, while detailed information on these compounds is presented in Supplementary Table S1 (Table S1) and Supplementary Figures (Figs. S3–S29).

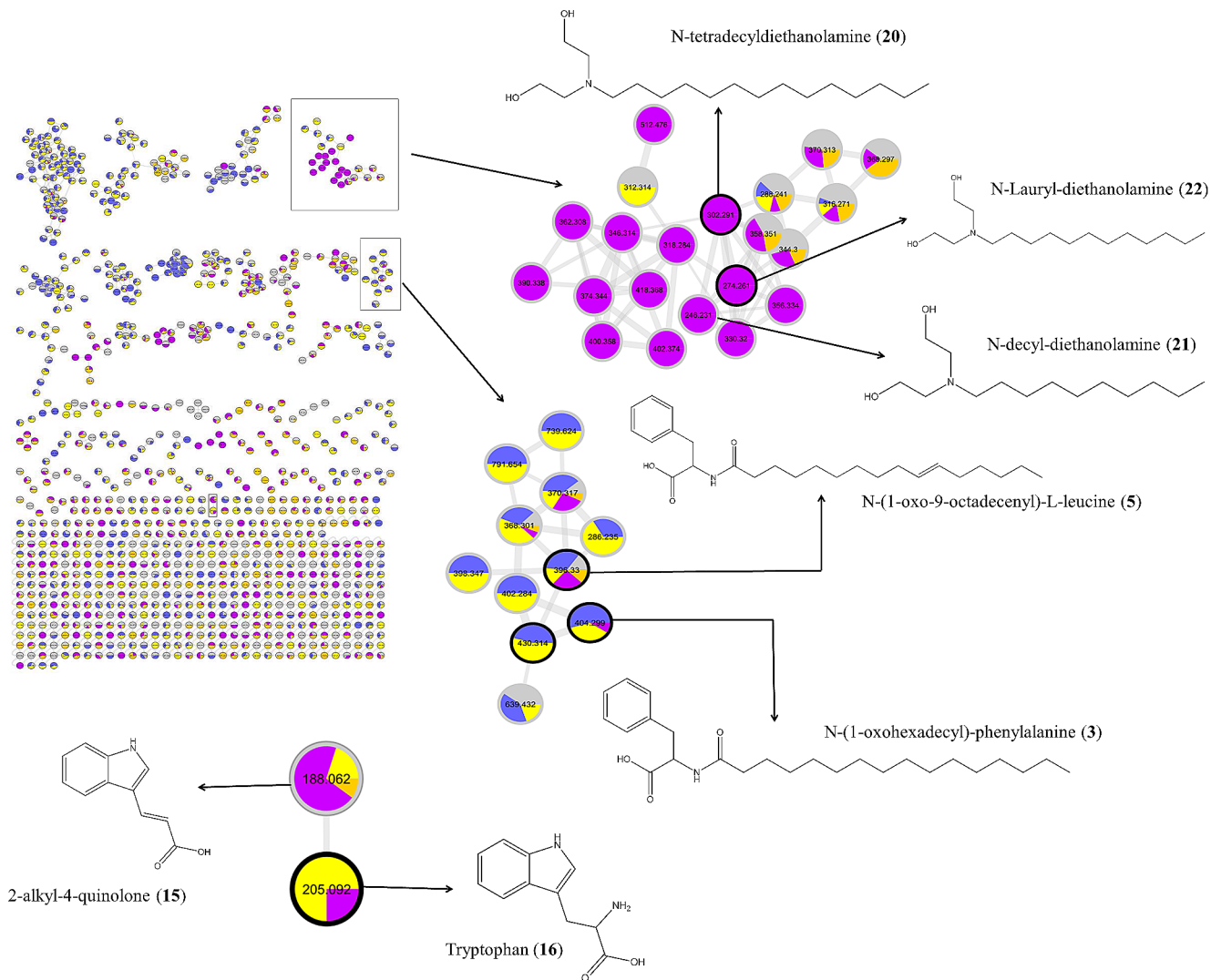


Fig. 2 Molecular Networking containing the main molecular families identified in the de-replication analysis of *Pantoea* sp. ELP04 using GNPS platform. Nodes with black border: substances annotated by GNPS. Nodes with gray color border: substances identified based on

spectral similarities, fragmentation profile, and literature. In Blue: *Pantoea* sp. non-irradiated (ethyl acetate); Yellow: *Pantoea* sp. irradiated (ethyl acetate); Purple: *Pantoea* sp. non-irradiated (methanol); Orange: *Pantoea* sp. irradiated (methanol)

A family of lipoamino acids was observed, including m/z 404.299 (N-(1-oxohexadecyl)-phenylalanine (3), m/z 396.33 (N-(1-oxo-9-octadecenyl)-leucine (5), m/z 402.284 (N-hexadec-9-enoylphenylalanine (1), m/z 370.317 (N-(1-oxohexadecyl)-leucine (4), and m/z 368.301 (N-(1-oxo-9-hexadecenyl)-leucine (7) (Fig. 2; Table 2, and Table S2). The ion with m/z 188.062 (2-alkyl-4-quinolone) (14) was also detected in the MeOH fraction of non-irradiated bacteria and the MeOH/EtOAc extract of irradiated bacteria (Fig. 2).

Ions with m/z 302.291 and m/z 274.261 were predominantly detected in MeOH fractions from non-irradiated bacteria and were identified as N-tetra decyl diethanolamine (18) and N-Lauryl diethanolamine (20), and clustered in the same family with other identified organic amines m/z 246.2428 (19), m/z 318.3008 (21), and m/z 346.3321 (22) (Fig. 2; Table 2, and Table S2). Eight other ions detected in this extract (m/z 362.308, m/z 346.314, m/z 390.338, m/z 374.344, m/z 418.368, m/z 330.320, m/z 400.358, and m/z 402.374) were also clustered in this family, indicating similarity with these substances (Fig. 2).

Molecular networking is used for the visualization and qualitative interpretation of spectroscopic data by identifying

possible similarities between MS/MS spectra within the dataset [17]. The analysis is based on the assumption that structurally related molecules have similar fragmentation patterns and, therefore, are related within a network [34].

The lipoamino acid networks of N-(1-oxohexadecyl)-phenylalanine (3), N-(1-oxo-9-octadecenyl)-leucine (5), N-hexadec-9-enoylphenylalanine (1), N-(1-oxohexadecyl)-leucine (4), and N-(1-oxo-9-hexadecenyl)-leucine (7) have previously been reported by Touré et al. [20]. Furthermore, analysis of the molecular networks verified that ionizing radiation does not negatively affect the production of secondary metabolites with biotechnological interest that are commonly produced by *Pantoea* sp., such as 3-indolepropionic acid (9), Tryptophol (10), and Tryptophan (24) [19]. It has already been demonstrated that exposure to gamma radiation can influence the production of auxin, notably indole-3-acetic acid [35].

Analysis of the EtOAc extract identified 17 compounds in the positive ionization mode and two compounds in the negative ionization mode. Based on these two modes, 80% of the ions were detected in both the non-irradiated (F2) and radiation-exposed cells (F3). Pyridindolol (12) and 1-hydroxy-4-methylcarbostyryl (13) were only detected in

Table 2 Chemical identification of secondary metabolites produced by *Pantoea* sp. ELP04 not exposed (F2) and exposed (F3) to gamma radiation. Exposure: 48 h, final dose: 1.45 Gy

Metabolite	Molecular formula	Extract		Ionization mode	Extract type
		F2	F3		
N-hexadec-9-enoyl-phenylalanine (1)	C ₂₅ H ₃₉ NO ₃	+	+	Positive	EtOAc
N-(1-oxotetradecyl)-phenylalanine methyl ester (2)	C ₂₄ H ₄₀ NO ₃	+	+	Positive	EtOAc
N-(1-oxohexadecyl)-phenylalanine (3)	C ₂₅ H ₄₁ NO ₃	+	+	Positive	EtOAc
N-(1-oxohexadecyl)-leucine (4)	C ₂₂ H ₄₃ NO ₃	+	+	Positive	EtOAc
N-(1-oxo-9-octadecenyl)-leucine (5)	C ₂₄ H ₄₅ NO ₃	+	+	Positive	EtOAc
N-(1-oxotetradecyl)-leucine (6)	C ₂₀ H ₄₉ NO ₃	+	+	Positive	EtOAc
N-(1-oxo-9-hexadecenyl)-leucine (7)	C ₂₂ H ₄₁ NO ₃	+	+	Positive	EtOAc
linolenic acid (8)	C ₁₈ H ₃₀ O ₂	+	+	Positive	EtOAc
3-indolepropionic acid (9)	C ₁₁ H ₁₁ NO ₂	+	+	Positive	EtOAc
Tryptophol (10)	C ₁₀ H ₁₁ NO	+	+	Positive	EtOAc
4-(hydroxymethyl)quinoline (11)	C ₁₀ H ₉ NO	+	+	Positive	EtOAc
Pyridindolol (12)	C ₁₄ H ₁₄ N ₂ O ₃	+	-	Positive	EtOAc
1-hydroxy-4-methylcarbostyryl (13)	C ₁₀ H ₉ NO ₂	+	-	Positive	EtOAc
2-alkyl-4-quinolone (14)	C ₁₂ H ₁₃ NO	+	+	Positive	EtOAc
5'-Methylthioadenosine (15)	C ₁₁ H ₁₅ N ₅ O ₃ S	-	+	Positive	EtOAc
Phenylpropanoic acid (16)	C ₉ H ₁₀ O ₂	+	+	Negative	EtOAc
Cinnamic acid (17)	C ₉ H ₇ O ₂	+	+	Negative	EtOAc
N-tetradecyl diethanolamine (18)	C ₁₈ H ₃₉ NO ₂	+	-	Positive	MeOH
N-decyl diethanolamine (19)	C ₁₄ H ₃₁ NO ₂	+	-	Positive	MeOH
N-Lauryl diethanolamine (20)	C ₁₆ H ₃₅ NO ₂	+	-	Positive	MeOH
N-2-dodecyl oxyethyl diethanolamine (21)	C ₁₈ H ₃₉ NO ₃	+	-	Positive	MeOH
N-2-tetradecyl oxyethyl diethanolamine (22)	C ₂₀ H ₄₃ NO ₃	+	-	Positive	MeOH
Tyrosine (23)	C ₉ H ₁₁ NO ₃	+	+	Positive	MeOH
Tryptophan (24)	C ₁₁ H ₁₂ N ₂ O ₂	+	+	Positive	MeOH

F2: metabolic extract obtained from control cells (not exposed to radiation); F3: extract obtained from cells exposed to ionizing radiation (48 h/1.45 Gy). (+) indicates presence and (-) absence in the evaluated extract

F2, while 5'-methylthioadenosine (15) was detected only in F3 (Table 2). Seven compounds in the MeOH extract were identified in the positive ionization mode (18–24) (Table 2).

Secondary metabolites derived from carbostyryl can inhibit or limit bacterial growth, often acting as enzyme inhibitors that block reactions in certain metabolic pathways [36–38]. Based on this, we hypothesize that 1-hydroxy-4-methylcarbostyryl may also act as an inhibitor or limiter of bacterial growth. Derivatives of monoalkyl ethers of triethanolamines, including compounds 18–22 described in Table 2, have antibacterial activity [39, 40]. Interestingly, these molecules were observed only in F2 extracts, indicating that gamma radiation can inactivate mechanisms involved in the control of cell growth in this isolate. However, this needs to be validated by analyzing genes involved in the metabolism of these molecules.

Pyridindolol (12) is synthesized by combining amino groups with aldehydes, a process catalyzed by enzymes known as Pictet-Spenglerase (*PSases*) [41]. However, the synthesis process has not been completely elucidated [42]. Blocking pseudouridimycin biosynthesis in *Streptomyces* sp. ID38640 led to the identification of a putative biosynthetic gene cluster for pyridindolol, which includes a *PSase*, FAD-binding oxidoreductase, and other key enzymes, and revealed that altered production levels of pyridindolol in various pseudouridimycin pathways (PUM) mutant strains [41–42]. Pyridindolol is produced by bacteria [43] and may act as a β -galactosidase inhibitor [44], thus impairing cellular metabolic pathways that are important for energy generation, including the breakdown of lactose into galactose and glucose. This suggests that this metabolite may play a role in the growth of *Pantoea* sp. ELP04 under the studied conditions, based on the results presented in Table 1 and Fig. S1.

In the absence of ionizing stress, metabolites, such as 1-hydroxy-4-methylcarbostyryl (13), may be produced and excreted into the culture medium by the bacteria, and their accumulation and combination with other factors in the stationary phase may limit bacterial growth. When exposed to ionizing radiation originating from ^{137}Cs , putative DNA damage caused by the radiation potentially impaired and/or interfered with its biosynthesis route, preventing its production and accumulation in the extracellular environment. This was not detected in F3. This did not interfere with bacterial growth but increased cell concentration (Table 1, Fig. S1).

The absence of Pyridindolol (12) in F3 cells suggests that DNA damage might affect the functionality, or the radiation affect the expression of genes or other genetic complexes involved in these biosynthesis pathways. Ionizing radiation can severely damage the genomes of organisms, causing DNA breaks and, consequently, death or mutations. Exposure to radiation can induce or repress multiple genes,

suggesting that gene regulation is important for developing resistance to ionizing radiation [45–48].

In *Pantoea ananatis*, carotenoids can promote resistance to toxoflavin and UV radiation, and their production is dependent on the stress response regulator *RpoS*, which is positively regulated by *Hfq/ArcZ* and negatively regulated by *ClpXP*, were the *Hfq* protein and its associated small RNAs, including *ArcZ*, play a crucial role in regulating this pathway [49].

Pal et al. [50] investigates the gamma irradiation resistance in *Metabacillus halosaccharovorans* (VITHBRA001) and *Bacillus paralicheniformis* (VITHBRA024) from high background radiation areas in Chavara-Neendakara, India. Key strategies of resistance include robust DNA repair mechanisms such as homologous recombination (RecFOR pathway), base excision repair (multiple glycosylases), and nucleotide excision repair (UvrABC, UvsE). Both strains manage oxidative stress through enzymes like catalases, superoxide dismutases, and peroxidases, and have systems for manganese/iron homeostasis involving Mn-uptake transporters and iron-sequestering proteins. Unique to VITHBRA001 are additional protective enzymes (e.g., *FrnE* gene) and secondary metabolites like C30 carotenoids, which likely contribute to its higher resistance. The results underscore gene redundancy and specialized metabolic pathways adapted to radiation stress, comparable to highly resistant *Deinococcus radiodurans* but distinct from more sensitive *Escherichia coli*. While the specific genetic responses of *Pantoea* bacteria to Cs^{137} radiation remain to be elucidated, the regulatory mechanisms and stress response pathways observed in related organisms may provide valuable clues for future studies.

5'-Methylthioadenosine (15), detected only in F3, is a hydrophobic sulfur-containing nucleoside that is found in both prokaryotic and eukaryotic cells [51]. In bacteria, one of the catabolic pathways of 5'-methylthioadenosine involves the degradation of adenine and 5-mitothio- α -D-ribose and its deamination to methylguanine [52]. This catabolic pathway may favor not only an increase in the replication of DNA molecules but also the translation processes, thus increasing energy production [53].

In eukaryotic cells, the 5'-Methylthioadenosine can be produced during polyamine metabolism, which is essential for cell growth [53–55]. Cells with enhanced pathways for polyamine synthesis and direct or indirect synthesis of 5'-methylthioadenosine show a high level of proliferation [53]. The presence of this nucleoside in the metabolic extract of irradiated *Pantoea* sp. ELP04, but not in the non-irradiated cell extract, may be correlated with the differential growth observed between these bacterial populations (Table 1 and Fig. S1). This observation, along with the other hypotheses raised, may offer insights into the mechanisms

underlying the growth disparity, without drawing a direct analogy to eukaryotic cells.

PCA was conducted using results from the UPLC-HRMS chromatograms of the EtOAc extract. Retention times and peaks obtained from the mass spectra were used to determine differences between EtOAc extracts of *Pantoea* sp. ELP04 bacterial cells exposed to radiation for 48 h (1.45 Gy) and cells that were not irradiated (Fig. 3).

PCA of data derived from the analysis of the positive (Fig. 3a) and negative (Fig. 3b) ion modes in the EtOAc extracts of F2 and F3 differed from those of F1, the control containing only the culture medium. Principal component 1 (PC1) showed similarities between F2 and F3, while PC2 showed differences between F2 and F3. Notably, the sample variability explained by PC2 in both analyses was relatively low, showing that the F2 and F3 extracts have few quantitative differences in relation to their variables.

A heatmap was generated to show the correlations between positive mode ions with greater importance in relation to the detected sample variability (Fig. 4a). Six ions in the metabolite extract from the irradiated bacteria (F3) had greater intensities than those from the non-irradiated control isolate (F2): m/z 208.0966 (4.11 min), m/z 353.2650 (10.93 min), m/z 485.3461 (8.16 min), m/z 567.2706 (4.04 min), m/z 355.3308 (90.09 min), and m/z 227.2001 (9.35 min). Five ions in the extract from the control isolate (F2) had greater intensities than metabolites from the

irradiated isolate (F3), with the ion at m/z 573.3983 (at 7.97 min) having the highest intensity (Fig. 4a).

Analysis of the negative mode identified 21 ions with great intensity in the extracts from irradiated bacteria, with ions with m/z 151.0255 (0.97 min), m/z 107.0493 (4.33 min), m/z 243.1954 (9.05 min), m/z 145.0498 (1.48 min), m/z 259.1897 (7.37 min), and m/z 159.0862 (4.82 min) having the highest intensities. The ion with m/z 332.1379 (identified at 5.40 min) had a lower intensity in the F3 extract than those in the F2 (non-irradiated bacteria) and F1 (control with culture medium) extracts. The m/z 329.2307 (6.63 min), m/z 131.0707 (4.07 min), and m/z 135.0294 (0.96 min) ions had greater intensities in the F2 extract than those in the F3 extract (Fig. 4b).

These results support the possibility of changes occurring in the metabolisms of the microorganisms involved in the radiotolerance process. However, it has not yet been determined whether these differences are due to genomic, epigenetic, or other alterations directly caused by gamma radiation itself. Additionally, the molecular network and multivariate analysis clearly show that the differences between irradiated and non-irradiated cultures are small, allowing us to propose that this could be an inherent mechanism of radiotolerance in these microorganisms rather than a random occurrence.

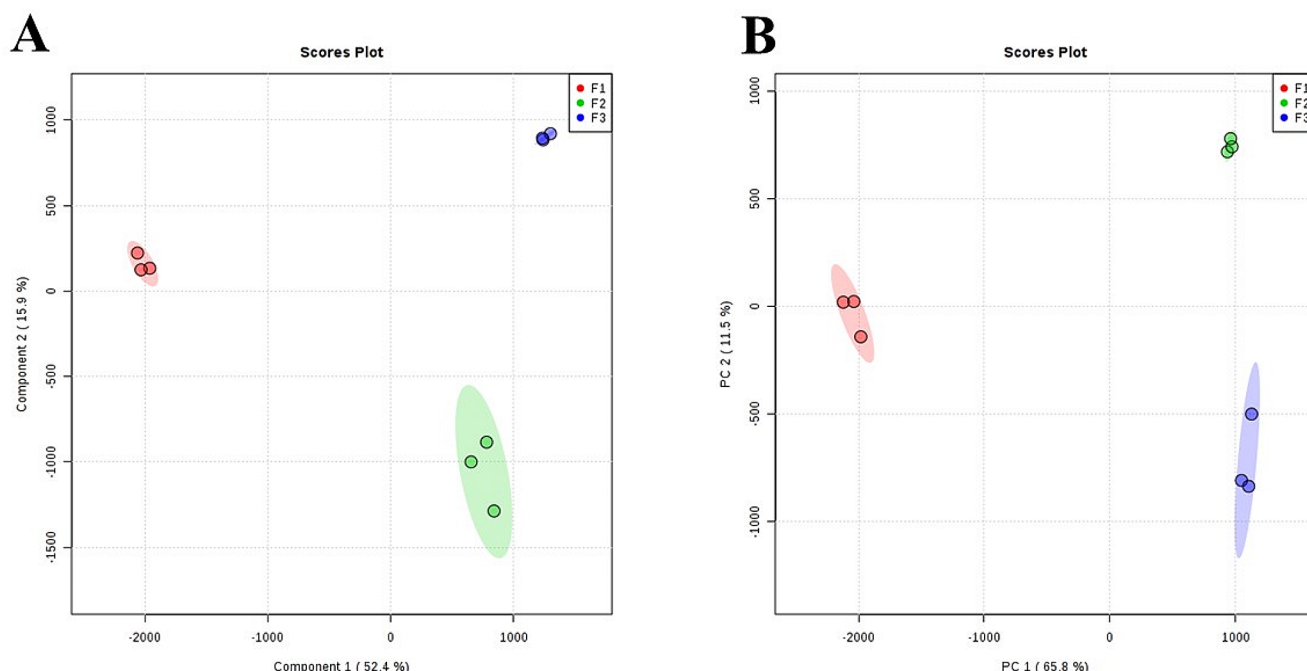


Fig. 3 Principal Component Analysis (PCA) of the extracts' spectral data produced by bacterial cells exposed and not exposed to radiation. In (A) positive ionization mode and in (B) negative ionization mode.

F1 = culture medium only with no microbial inoculum, F2 = bacteria non-irradiated, and F3 = irradiated bacteria for 48 h

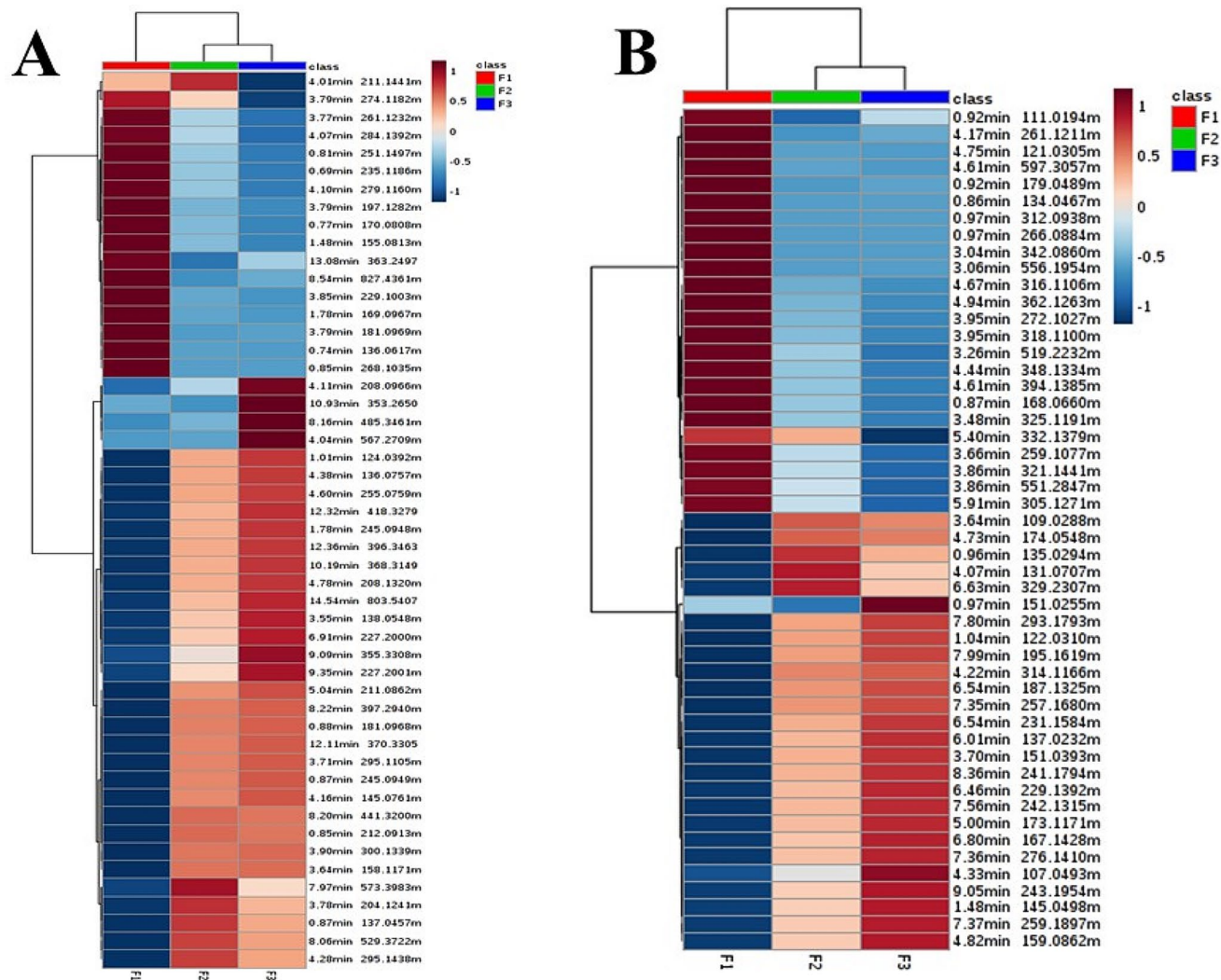


Fig. 4 Heatmap for positive ionization mode (A) and negative ionization mode (B). F1 = culture medium only with no microbial inoculum, F2 = non-irradiated bacteria, and F3 = irradiated bacteria for 48 h. The

greater the intensity for a detected ion, the redder the tone. In contrast, the smaller the intensity, the bluer the tone

Conclusion

In this study, we report, for the first time, on the sensitivity of the endophytic bacterium *Pantoea* sp. to ^{137}Cs gamma radiation. After 48 h, we observed an increase of 6 Log CFU.mL $^{-1}$ in the growth of irradiated bacteria compared with the non-irradiated control. Although there were no differences in microbial growth after 24 h of radiation exposure, non-irradiated bacteria produced compounds that potentially inhibited growth after 9 h of incubation, including 1-hydroxy-4-methylcarbostyryl (13), triethanolamine derivatives (18–22), and Pyridindolol (12). These metabolites were not detected in irradiated bacteria. 5'-Methylthioadenosine (15), which is produced by the bacteria following exposure to ionizing radiation, may be used as an indicator of radioresistance.

Chemometric analyses and molecular networking revealed some variations between the F2 and F3 samples; however, these results suggest that the metabolic profile of the irradiated bacteria at such doses remained relatively stable under both conditions, indicating that radiation minimally affects their metabolomes and, consequently, the integrity of their genomes. This is important when considering that this endophyte can produce other compounds of biotechnological interest even after exposure to radiation.

Overall, our results are significant because they, along with future investigations, may aid in the development of new strategies for generating materials and molecules from endophytic bacteria for radiological protection or bioremediation of radionuclides.

Supplementary Information The online version contains supplementary material available at <https://doi.org/10.1007/s42770-024-02070-1>

024-01458-z.

Acknowledgements We would like to dedicate this work to Prof. Dr. João Alencar Pamphile, who sadly passed away from COVID-19. We are extremely grateful for his contributions, and he has our affection, love, and admiration. Rest in peace! We would also like to thank the State University of Maringá, COMCAP, and CAPES (Coordination for the Improvement of Higher Education Personnel - Financial Code: 001) for the scholarships.

Author contributions J.A. dos S.O.: Conceptualization, Investigation, Methodology, Data curation, Formal analysis, Writing original draft. A.D.P.: Investigation, Methodology, Formal analysis. A.P.F.: Investigation, Methodology. N.B.L.: Investigation, Methodology, Formal analysis. C.A.M.: Methodology, Formal analysis. V.E.P.V.: Methodology, Formal analysis, Writing - review & editing. J.C.P.: Methodology, Data curation, Formal analysis, Validation, Writing - review & editing. A.V.G.R.: Methodology, Data curation, Formal analysis, Writing - review & editing. D.C.B.: Methodology, Formal analysis, Validation, Writing - review & editing. J.A.P.: Conceptualization, Supervision, Funding acquisition, Project administration. J.L.A.: Supervision, and Project Administration.

Funding This study was supported by CAPES (Coordenação de Aperfeiçoamento de Pessoal de Nível Superior) through scholarships (Finance code 001).

Data availability The datasets generated during and/or analysed during the current study are available from the corresponding author on reasonable request <https://zenodo.org/doi/10.5281/zenodo.12811285>.

Declarations

Competing Interests The authors declare that they have no conflict of interest.

References

1. Kambayashia S, Zhang J, Narita H (2021) Significance of Fukushima-derived radiocaesium flux via river-estuary-ocean system. *Sci Total Environ* 793:148456. <https://doi.org/10.1016/j.scitotenv.2021.148456>
2. Duong VH, Nguyen Thanh D, Bui LV, Kim TT, Duong TD, Hoang DH, Musthafa MS, Nguyen QH, Kovacs T, Tran HN (2021) Characteristics of radionuclides in soil and tea plant (*Camellia sinensis*) in Hoa Binh, Vietnam. *J Radioanal Nucl Chem* 329:805–814. <https://doi.org/10.1007/s10967-021-07850-5>
3. López-Pérez M, Martín-Luis C, Hernández F, Liger E, Fernández-Aldecoa JC, Lorenzo-Salazar JM, Hernández-Armas J, Salazar-Carballo PA (2021) Natural and artificial gamma-emitting radionuclides in volcanic soils of the Western Canary Islands. *J Geochem Explor* 229:106840. <https://doi.org/10.1016/j.gexplo.2021.106840>
4. Ritchie JC, McHenry JR (1990) Application of Radioactive Fallout Cesium-137 for Measuring Soil Erosion and Sediment Accumulation Rates and patterns: a review. *J Environ Qual* 19:215–233
5. Fuini SC, Souto R, Amaral GF, Amaral RG (2013) Quality of life in individuals exposed to cesium-137 in Goiânia, Goiás State, Brazil. *Cad Saúde Pública* 29(7):1301–1310. <https://doi.org/10.1590/s0102-311x2013000700005>
6. Webb KM, Diruggierom J (2012) Role of Mn²⁺ and compatible solutes in the Radiation resistance of thermophilic Bacteria and Archaea. *Archaea* 2012(845756). <https://doi.org/10.1155/2012/845756>
7. Nayak T, Sengupta I, Dhal PK (2021) A new era of radiation resistance bacteria in bioremediation and production of bioactive compounds with therapeutic potential and other aspects: an in-perspective review. *J Environ Radioact* 237:106696. <https://doi.org/10.1016/j.jenvrad.2021.106696>
8. Singh OV, Gabani P (2011) Extremophiles: radiation resistance microbial reserves and therapeutic implications. *J Appl Microbiol* 110:851–861. <https://doi.org/10.1111/j.1365-2672.2011.04971.x>
9. Gabani P, Singh OV (2013) Radiation-resistant extremophiles and their potential in biotechnology and therapeutics. *Appl Microbiol Biotechnol* 97:993–1004. <https://doi.org/10.1007/s00253-012-4642-7>
10. Kusari S, Singh S, Jayabaskaran C (2014) Biotechnological potential of plant-associated endophytic fungi: hope versus hype. *Trends Biotechnol* 32(6):297–303. <https://doi.org/10.1016/j.tibtech.2014.03.009>
11. Emmer A, Oliveira JAS, Polli AD, Polonio JC, Alves LH, Fávaro-Polonio CZ, Azevedo JL, Pamphile JA (2021) Plant growth-promoting activity in bean plants of endophytic bacteria isolated from *Echeveria Laui*. *Acta Brasiliensis* 5(2):65–71
12. Santos CM, Ribeiro AS, Garcia A, Polli AD, Polonio JC, Azevedo JL, Pamphile JA (2019) Enzymatic and antagonist activity of endophytic fungi from *Sapindus saponaria* L. (Sapindaceae). *Acta Biol Colomb* 24(2): 322–330. <https://doi.org/10.15446/abc.v24n2.74717>
13. Silva AA, Polonio JC, Oliveira JAS et al (2020) Multilocus sequence analysis of endophytic fungi from *Justicia brandegeana* with the culture-dependent method and their bioprospection for health field. *S Afr J Bot* 134:359–368. <https://doi.org/10.1016/j.sajb.2020.05.007>
14. Hiago M, Kang DJ, Isobe K (2019) First report of community dynamics of arbuscular mycorrhizal fungi in radiocesium degradation lands after the Fukushima-Daiichi Nuclear disaster in Japan. *Sci Rep* 9:8240. <https://doi.org/10.1038/s41598-019-44665-7>
15. Ahsan MT, Najam-ul-haq M, Idrees M, Ullah I, Afzal M (2017) Bacterial endophytes enhance phytostabilization in soils contaminated with uranium and lead. *Int J Phytorem* 19(10):937–946. <https://doi.org/10.1080/15226514.2017.13038>
16. Oliveira JAS, Polli AD, Polonio JC, Orlandelli RC, Conte H, Azevedo JL, Pamphile JA (2020) Bioprospection and molecular phylogeny of culturable endophytic fungi associated with yellow passion fruit. *Acta Sci Biol Sci* 42:e48321. <https://doi.org/10.4025/actascibiolsci.v42i1.48321>
17. Wang M, Carver JJ, Phelan VV et al (2016) Sharing and community curation of mass spectrometry data with Global Natural products Social Molecular networking. *Nat Biotechnol* 34:828–837. <https://doi.org/10.1038/nbt.3597>
18. Shannon P, Markiel A, Ozier O et al (2003) Cytoscape: a software environment for integrated models of biomolecular interaction networks. *Genome res* 13(11):2498–2504. <https://doi.org/10.1101/gr.123930>
19. Rustamova N, Bobakulov K, Begmatov N, Turak A, Yili A, Aisa HA (2021) Secondary metabolites produced by endophytic *Pantoea ananatis* derived from roots of *Baccharoides Anthelmintica* and their effect on melanin synthesis in murine B16 cells. *Nat Prod Res* 35(5):796–801. <https://doi.org/10.1080/14786419.2019.1597354>
20. Touré S, Desrat S, Pellissier L et al (2019) Characterization, diversity, and structure-activity relationship study of lipoamino acids from *Pantoea* sp. and synthetic analogues. *Int J Mol Sci* 20:1083. <https://doi.org/10.3390/ijms20051083>
21. Morin A, Parveen Z (1999) Pantoea. *Encyclopedia Food Microbiol* 1623–1630. <https://doi.org/10.1006/rwfm.1999.1220>

22. Rosén K, Weiliang Z, Mårtensson A (2005) Arbuscular mycorrhizal fungi mediated uptake of ^{137}Cs in leek and ryegrass. *Sci Total Environ* 338:283–290. <https://doi.org/10.1016/j.scitotenv.2004.07.015>

23. Dubchak S, Ogar A, Mietelski JW, Turnau K (2010) Influence of silver and titanium nanoparticles on arbuscular mycorrhiza colonization and accumulation of radiocesium in *Helianthus annuus*. *Span J Agri Res* 8(1):103–108

24. Gyuricza V, Declerck S, De Dupré H (2010) Arbuscular mycorrhizal fungi decrease radiocesium accumulation in *Medicago truncatula*. *J Environ Radioact* 101:591–596. <https://doi.org/10.1016/j.jenvrad.2010.03.004>

25. Ben Salem I, Sghaier H, Monsieurs P, Moors H, Van Houdt R, Fattouch S, Saidi M, Landolsi A, Leys N (2013) Strontium-induced genomic responses of *Cupriavidus metallidurans* and strontium bioprecipitation as strontium carbonate. *Ann Microbiol* 63(3):833–844. <https://doi.org/10.1007/s13213-012-0462-3>

26. Bousselmi M, Mustapha MB, Khamessi M, Abelli W, Saidi M, Fattouch S (2016) Isolation and Characterisation of a Novel Radioresistant Bacteria from *Phosphogypsum* in Tunisia. *IJIR* 2: 2454–1362

27. Zavilgelsky GB, Abilev SK, Sukhodolets VV, Ahmad SI (1998) Isolation and analysis of UV and radio-resistant bacteria from Chernobyl. *J Photochem Photobiol B: Biol* 43:152–157

28. Fredrickson JK, Zachara JM, Balkwill DL, Kenedy D, Li S-MW, Kostandarithes HM, Daly M, Romine MF, Brockman FJ (2004) Geomicrobiology of High-Level Nuclear Waste-contaminated vadose sediments at the Hanford Site, Washington State. *Appl Environ Microbiol* 70:4230–4241. <https://doi.org/10.1128/aem.70.7.4230-4241.2004>

29. Romanovskaya VA, Rokitko PV, Mikheev AN, Gushcha NI, Malashenko YR, Chernaya NA (2002) The effect of g-Radiation and Desiccation on the viability of the soil Bacteria isolated from the Alienated Zone around the Chernobyl Nuclear Power Plant. *Microbiol* 71(5):608–613. <https://doi.org/10.1023/A:1020575223365>

30. Choudhary S, Sar P (2011) Identification and characterization of uranium accumulation potential of a uranium mine isolated *Pseudomonas* strain. *World J Microbiol Biotechnol* 27:1795–1801. <https://doi.org/10.1007/s11274-010-0637-7>

31. Shuryak I (2019) Review of microbial resistance to chronic ionizing radiation exposure under environmental conditions. *J Environ Radioact* 196:50–63. <https://doi.org/10.1016/j.jenvrad.2018.10.012>

32. Kuwahara C, Fukumoto A, Nishina M, Sugiyama H, Anzai Y, Kato F (2011) Characteristics of cesium accumulation in the filamentous soil bacterium *Streptomyces* sp. K202. *J Environ Radioact* 102(2):138–144. <https://doi.org/10.1016/j.jenvrad.2010.11.004>

33. Prione LP, Olchanheski LR, Tullio LD et al (2016) Gst activity and membrane lipid saturation prevents mesotrione-induced cellular damage in *Pantoea ananatis*. *AMB Expr* 6:70. <https://doi.org/10.1186/s13568-016-0240-x>

34. Quinn RA, Nothias LF, Vining O, Meehan M, Esquenazi E, Dorestein PC (2017) Molecular networking as a drug discovery, drug metabolism, and precision medicine strategy. *Trends Pharmacol Sci* 38:143–154. <https://doi.org/10.1016/j.tips.2016.10.011>

35. Lage CLS, Esquivel MA (1995) Role of non enzymatic synthesis of indole-3-acetic acid in the Ipomoea batatas L.Lam. (sweet potato) response to gamma radiation. *Arq Biol Tecnol* 38(4):1173–1180

36. Taniguchi M, Satomura Y (1972) Structure and physiological activity of Carbostyryl compounds. *Agr Bio Chem* 36(12):2169–2175

37. Tashima T (2015) The structural use of carbostyryl in physiologically active substances. *Bioorg Medic Chem Lett* 25:3415–3419. <https://doi.org/10.1016/j.bmcl.2015.06.027>

38. Hariguchi N, Chen X, Hayashi Y et al (2020) OPC-167832, a Novel Carbostyryl Derivative with Potent Antituberculosis Activity as a DprE1 inhibitor. *Antimicrob Agents Chemother* 64(6):e02020–e02019. <https://doi.org/10.1128/AAC.02020-19>

39. Sturm H, Konermann E, Aeschbacher R, Gradmann R (1953) Quaternary ammonium compounds with bactericidal properties. *Ind Eng Chem* 45:186–187

40. Vadla NC, Davalagar VD, Sripadi P (2013) Detection and characterization of N-alkyl diethanolamines and N-2-alkoxyethyl diethanolamines in milk by electrospray ionization mass spectrometry. *Metabolomics* 9:623–630. <https://doi.org/10.1007/s11306-012-0492-7>

41. Roddan R, Ward JM, Keep NH, Hailes HC (2020) Pictet-spenglerases in alkaloid biosynthesis: future applications in biocatalysis. *Curr Opin Chem Biol* 55:69–76. <https://doi.org/10.1016/j.cbpa.2019.12.003>

42. Iorio M, Davatgarbenam S, Serina S et al (2021) Blocks in the pseudouridimycin pathway unlock hidden metabolites in the *Streptomyces* producer strain. *Sci Rep* 11:5827. <https://doi.org/10.1038/s41598-021-84833-2>

43. Aoyagi T, Kumagai M, Hazato T, Mamada M, Takeuchi T (1975) Pyridindolol, a new β -galactosidase inhibitor produced by actinomycetes. *J Antibiot* 28:555–557. <https://doi.org/10.7164/antibiotics.28.555>

44. Kumagai M, Aoyagi T, Umezawa H (1976) Inhibitory activity of pyridindolol on β -galactosidase. *J Antibiot* 29(7):696–703. <https://doi.org/10.7164/ANTIBIOTICS.29.696>

45. Blanchard L, Guérin P, Roche D, Cruveiller S, Pignol D, Vallenet D, Armengaud A, de Groot A (2017) Conservation and diversity of the IrrE/DdrO-controlled radiation response in radiation-resistant *Deinococcus* bacteria. *Microbiol Open* 6(4):e00477. <https://doi.org/10.1002/mbo3.477>

46. Wang W, Ma Y, He J, Qi H, Xiao F, He S (2016) Gene regulation for the extreme resistance to ionizing radiation of *Deinococcus radiodurans*. *Gene* 715:144008. <https://doi.org/10.1016/j.gene.2019.144008>

47. Yang S, Xu H, Wang J et al (2016) Cyclic AMP receptor protein acts as a transcription regulator in response to stresses in *Deinococcus radiodurans*. *PLoS ONE* 11(5):e0155010. <https://doi.org/10.1371/journal.pone.0155010>

48. Meyer L, Coste G, Sommer S, Oberto J, Confalonieri F, Servant P, Pasternak C (2018) DdrI, a cAMP receptor protein family Member, acts as a Major Regulator for Adaptation of *Deinococcus radiodurans* to various stresses. *J Bacteriol* 200(13):e00129–e00118. <https://doi.org/10.1128/JB.00129-18>

49. Choi O, Kang B, Lee Y, Lee Y, Kim J (2021) *Pantoea ananatis* carotenoid production confers toxoflavin tolerance and is regulated by hfq-controlled quorum sensing. *MicrobiologyOpen* 10(1):e1143. <https://doi.org/10.1002/mbo3.1143>

50. Pal S, Yuvaraj R, Krishnan H, Venkatraman B, Abraham J, Gopinathan A (2024) Unraveling radiation resistance strategies in two bacterial strains from the high background radiation area of Chavara-Neendakara: a comprehensive whole genome analysis. *PLoS ONE* 19(6):e0304810. <https://doi.org/10.1371/journal.pone.0304810>

51. Avila MA, Garcia-Trevijano ER, Lu SC, Corrales FJ, Mato JM (2004) Methylthioadenosine. *Int J Biochem Cell Biol* 36:2125–2130. <https://doi.org/10.1016/j.biocel.2003.11.016>

52. Guan R, Ho MC, Frohlich RF, Tyler PC, Almo SC, Schramm VL (2012) Methylthioadenosine deaminase in an alternative quorum sensing pathway in *Pseudomonas aeruginosa*. *Biochemistry* 51:9094–9103. <https://doi.org/10.1021/bi301062y>

53. Li Y, Wang Y, Wu P (2019) 5'-Methylthioadenosine and Cancer: old molecules, new understanding. *J Cancer* 10(4):927. <https://doi.org/10.7150/jca.27160>

54. Williams-Ashman HG, Seidenfeld J, Galletti P (1982) Trends in the biochemical pharmacology of 5'-deoxy-5'-methylthioadenosine. *Biochem Pharmacol* 31:277–288. [https://doi.org/10.1016/0006-2952\(82\)90171-x](https://doi.org/10.1016/0006-2952(82)90171-x)
55. Stevens AP, Dettmer K, Kirovski G et al (2010) Quantification of intermediates of the methionine and polyamine metabolism by liquid chromatography-tandem mass spectrometry in cultured tumor cells and liver biopsies. *J Chromatogr A* 1217:3282–3288. <https://doi.org/10.1016/j.chroma.2010.01.025>

Publisher's Note Springer Nature remains neutral with regard to jurisdictional claims in published maps and institutional affiliations.

Springer Nature or its licensor (e.g. a society or other partner) holds exclusive rights to this article under a publishing agreement with the author(s) or other rightsholder(s); author self-archiving of the accepted manuscript version of this article is solely governed by the terms of such publishing agreement and applicable law.